Evaluation of Simultaneous Localization and Calibration of a Train Mounted Magnetometer

Benjamin Siebler, *German Aerospace Center, Institute of Communications and Navigation (DLR-ICN)*
Andreas Lehner, *German Aerospace Center, Institute of Communications and Navigation (DLR-ICN)*
Stephan Sand, *German Aerospace Center , Institute of Communications and Navigation (DLR-ICN)*
Uwe D. Hanebeck, *Karlsruhe Institute of Technology (KIT), Intelligent Sensor-Actuator-Systems Laboratory (ISAS)*

BIOGRAPHY

Benjamin Siebler received his M.Sc. in electrical engineering and information technology from the KIT in 2014 and is currently pursuing his PhD at the Intelligent Sensor-Actuator-Systems Laboratory of the KIT. Since 2014 he is a researcher at the DLR-ICN with focus on multisensor localization with inertial sensors and magnetic field distortions.

Andreas Lehner received his Ph.D. from University Erlangen-Nuremberg in 2008. Since 2002 he is researcher at DLR-ICN focusing on GNSS multipath characterization, robust multi-sensor localization and decentralized wireless communication for land-mobile applications. Andreas has authored and co-authored more than 100 publications and co-founded Intelligence on Wheels GmbH in 2012.

Stephan Sand received his Ph.D. from ETH Zurich, Switzerland in 2010. Since 2002 Stephan has researched wireless communications and multi-sensor navigation at DLR-ICN. Since 2014 he is leading the Vehicular Applications Group researching robust navigation and wireless communications technologies for road users and railways. Stephan has authored and co-authored more than 100 publications.

Uwe D. Hanebeck is full professor at the KIT and director of the ISAS Laboratory. He obtained his Ph.D. degree and his habilitation degree in Electrical Engineering from the Technical University in Munich, in 1997 and 2003, respectively. His research interests are information fusion, nonlinear state estimation, stochastic modeling, system identification, and control. He is author and coauthor of more than 500 publications and an IEEE Fellow.

ABSTRACT

Train localization is a key technology for automating railway traffic and using the railway infrastructure efficiently. Localization must be available independent from the environment and must provide a high accuracy and reliability. A single localization solution most likely will not be able to fulfill this requirement. GNSS for example will not be available in tunnels. In this paper, we therefore investigate an alternative localization method based on position-dependent distortions of the Earth magnetic field. The advantage of this approach is that it is also available in GNSS-denied areas. If GNSS is available, it can be seen as a low-cost method to obtain redundant position information. The work presented here is an evaluation of the algorithm proposed in our prior work [1], in which we showed how an uncalibrated magnetometer can be used to simultaneously estimate the position of a model train and the magnetometer calibration parameters. The evaluation presented in this paper applies the simultaneous localization and calibration algorithm to data measured with two different trains driving on a rural track network in Germany. The evaluation shows that magnetic field based localization using only an uncalibrated magnetometer is also possible in real railway environments.

I. INTRODUCTION

Traditional operation procedures in railway traffic require two trains to be separated by the absolute braking distance at all times. For high-speed trains this means the trains have to be separated by several kilometers. It is apparent that this leads to an inefficient use of tracks and a low capacity in the network. While in rural areas this might be acceptable, in urban areas this causes delays and creates a bottleneck. In the future, it is therefore desirable to reduce the distance between trains below the absolute braking distance. Without accurate real time position information of all trains in the vicinity, this is hard to achieve as the large braking distances make it impossible to adapt the speed of an approaching train in time. This is in contrast to road vehicles, were it is usually sufficient to observe the environment of the own vehicle, e.g., with cameras or radars, to maintain a safe operation. For trains information beyond the measurement range of radars and cameras is required. Furthermore a direct distance measurement between different trains, if possible, can result in distances much smaller than the true distance due to the track geometry. The current solution to obtain train positions is the deployment of dedicated infrastructure, which is costly and prone to vandalism and theft. Therefore, it is desired to have a low-cost infrastructure-less alternative. A common choice to

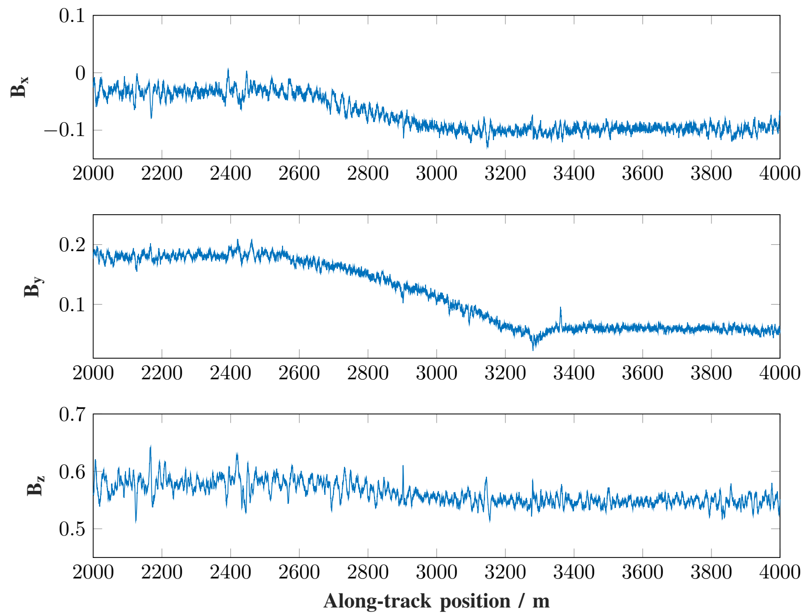

Figure 1: Example of the three components B_x,B_y and B_z of the magnetic field observed on a $2000\,\mathrm{m}$ long track segment in a rural area. The shown values are normalized by the sensor used during mapping. A value of 1 corespondents to approximately $40\,\mu\mathrm{T}$.

solve the localization problem is the use of global navigation satellite systems (GNSS) like GPS, Galileo, and GLONASS [2]. GNSS is a good choice in many environments but is vulnerable to jamming, spoofing, and shadowing. While jamming and spoofing are man-made and might be encountered only rarely, shadowing is encountered regularly and will lead to a reduced performance and availability. An extreme example is a tunnel, in which GNSS signals are completely blocked. But also in urban canyons the visibility of satellites can be dramatically reduced. If shadowing is only encountered for short periods, GNSS can be aided with an inertial navigation system (INS). Depending on the quality of the inertial sensors used in the INS, outages of a couple of seconds up to minutes can be bridged while maintaining a certain position accuracy. For longer outages, an INS has to have a very high quality that comes with considerable costs. We therefore proposed in our prior work [3, 4] the use of position-dependent distortions of the Earth magnetic field for train position estimation. This magnetic distortions are mainly caused by the existing railway infrastructure, particular the components containing ferromagnetic material like steel. If a map of the magnetic distortions for the whole track network it created it is possible to localize a train in the network by comparing the measurements of a low-cost on-board magnetometer with the mapped magnetic field. One of the main issues in performing magnetic localization is the calibration of the magnetometers. The magnetometer measurements are affected by the ferromagnetic material in its vicinity. This means that a sensor placed in the same height and the same lateral position relative to the track but in a different train will measure a different magnetic field. Therefore the sensor requires calibration. Common procedures for magnetometer calibration require the sensor and the platform it is mounted on to be rotated in a homogenous magnetic field. If the platform is a train this is not possible without considerable effort. An alternative would be to create a known but varying magnetic field around the train. Due to the large volume of the train this also requires considerable effort and costs. In [1] we therefore proposed an algorithm that allows to estimate the calibration parameters simultaneously with the train position. The main idea is that instead of creating an artificial magnetic field around the train, the train can also move through the inhomogeneous field of the railway environment that is known from a prior created map. If the train position is known, calibration becomes trivial since for each magnetometer measurement the true magnetic field can be found from the map. Since the primary interest here is the train position, this can not be assumed. Therefore the position and calibration parameters are estimated at the same time in a Bayesian filter. In [1] the feasibility of this algorithm was shown with measurements of a model train driving in a laboratory of the German Aerospace Center. In this paper we now show that the algorithm also works for real trains and that estimating the calibration parameters simultaneously with the position results in a high position accuracy.

II. MAGNETIC FIELD IN THE RAILWAY ENVIRONMENT

The magnetic field along a railway track is distorted by the ferromagnetic material surrounding it. Such material is found in the rails, poles for power lines, and signals but also in steel reinforced concrete in bridges, buildings, and sound barriers. All this material combined influences the Earth magnetic field that is otherwise almost homogeneous in areas with a certain extent. In our investigation we found that the resulting distorted magnetic field contains sufficient variability and therefore information to estimate the train position solely using measurements of a magnetometer [3]. These distortions are also encountered in other environments, e.g., inside buildings due to steel reinforced concrete and metal beams [5]. An example of the magnetic field along a $2000\,\mathrm{m}$ long track segment of the Harzer Schmalspurbahnen (HSB) is shown in Fig. 1. The magnetic field contains position- and heading-dependent information. At roughly along-track position $2600\,\mathrm{m}$ the train is driving in a curve, which results in a significant change in the measured average magnetic field in the magnetometer axis in the horizontal plane due to the heading change. This effect is typically utilized in an electronic compass to find the north direction. In addition to the change of the average level, changes with a smaller amplitude and higher spatial frequency are observed. These smaller changes allow to localize the train with a higher accuracy than the heading-induced changes. In [6] it was shown that by using only the magnetic field a root-mean-square-error (RMSE) around $5\,\mathrm{m}$ compared to the position estimated by a single frequency GPS receiver is achievable. In [4] additionally a single accelerometer and a more robust filtering algorithm was used to estimate the train position and the switchway.

III. SIMULTANEOUS LOCALIZATION AND CALIBRATION

1. Magnetometer Calibration

The magnetometer under consideration in this paper has three orthogonal axes. This enables the sensor to measure the direction and amplitude of the magnetic field at the current position. One of the difficulties in measuring the magnetic field is caused by the disturbance from nearby magnetic material. If the same sensor is placed on two different positions in the same train, while maintaining the same height and lateral position relative to the track, one would expect the sensors to measure the same magnetic field. But this is most likely not true due to soft and hard iron effects caused by different magnetic material in the train at different mounting positions. Hard iron effects will cause an offset in the measured magnetic field vector. In contrast, soft iron effects will result in a rotation and scaling of the measured magnetic field. Mathematically these two effects result in a single linear transformation of the true magnetic field [7] encountered at a certain position of the train on the track

$$\tilde{\mathbf{z}}_k^b = \mathbf{C}\mathbf{R}_n^b(k)\mathbf{z}_k^n + \mathbf{b} + \mathbf{n}_k, \tag{1}$$

where $\tilde{\mathbf{z}}_k^b$ is the measured magnetic field in the sensor's body frame at the discrete time step k, $\mathbf{z}_k^n$ the true magnetic field in the navigation frame (the navigation frame is here attached to the track), $\mathbf{R}_n^b(k)$ is the rotation matrix from navigation to body frame, $\mathbf{C} \in \mathbb{R}^{3\times 3}$ a matrix accounting for the soft iron effects, $\mathbf{b} \in \mathbb{R}^3$ the offset vector of the hard iron effects, and $\mathbf{n}_k \sim \mathcal{N}(\mathbf{0}, \sigma^2\mathbf{I}_{3\times 3})$ is the measurement noise of the magnetometer.

After defining the sensor model, calibration can be performed with a simple linear least-squares estimator (LSE). This becomes clearer when (1) is rewritten as a function of a single parameter vector comprising the elements of $\mathbf{C}$ and $\mathbf{b}$

$$\begin{aligned}\tilde{\mathbf{z}}_k^b &= \mathbf{H}(\mathbf{R}_n^b(k)\mathbf{z}_k^n)\boldsymbol{\theta} + \mathbf{n}_k \\ &= \mathbf{H}(\mathbf{z}_k^b)\boldsymbol{\theta} + \mathbf{n}_k\end{aligned} \tag{2}$$

where $\mathbf{z}_k^b$ is the value a calibrated sensor should measure, $\mathbf{H}$ is a matrix

$$\mathbf{H}(\mathbf{z}_k^b) = \begin{bmatrix} (\mathbf{z}_k^b)^T & \mathbf{0}_{1\times 3} & \mathbf{0}_{1\times 3} & 1 & 0 & 0 \\ \mathbf{0}_{1\times 3} & (\mathbf{z}_k^b)^T & \mathbf{0}_{1\times 3} & 0 & 1 & 0 \\ \mathbf{0}_{1\times 3} & \mathbf{0}_{1\times 3} & (\mathbf{z}_k^b)^T & 0 & 0 & 1 \end{bmatrix} \tag{3}$$

and $\boldsymbol{\theta} \in \mathbb{R}^{12}$ is the parameter vector

$$\boldsymbol{\theta} = \begin{bmatrix} c_1 & c_2 & c_3 & \mathbf{b}^T \end{bmatrix}^T, \tag{4}$$

where c_i is the i-th row of matrix $\mathbf{C}$. Equation (2) is clearly linear in $\boldsymbol{\theta}$ and therefore can be estimated by a linear LSE. The parameter vector has dimension twelve and a single measurement in the sensors body frame $\tilde{\mathbf{z}}^b$ has dimension three. Hence at least four different measurements are required. For a good estimate in practice one will use more measurements because only noisy measurements are available.

The main problem encountered when the magnetometer is mounted on a train is to obtain the magnetic field $\mathbf{z}_k^b = \mathbf{R}_n^b(k)\mathbf{z}_k^n$ a calibrated sensor is supposed to measure because the rotation matrix $\mathbf{R}_n^b(k)$ and the magnetic field $\mathbf{z}_k^n$ may continuously change along a railway track. To obtain the correct value, three quantities are required:

1. Along track position s_k of the train on the track at time step k, or to be more precise, the position of the magnetometer
2. Map function $\mathrm{m}^n(s_k)$ of the magnetic field along the railway track that returns the magnetic field for each position
3. Rotation matrix $\mathbf{R}_n^b(k)$ between the navigation frame and the body frame of the sensor at time step k

In this paper, the map is assumed to be given. The map creation is a different problem that might require a measurement train for GNSS denied areas that is equipped with additional, possible costly, sensors to perform some sort of simultaneous localization and mapping (SLAM). The map creation therefore requires some effort but once the map is created the method presented in the next section enables the localization of different types of trains solely with a low-cost three-axis magnetometer.

For calibration, we still need to know the rotation matrix $\mathbf{R}_n^b(k)$ and the current train position. Position estimation will be explained in the next section and will be considered as given in this section. For the rotation matrix between navigation and body frame we observe that a train driving on a track will always be aligned with the pitch and yaw angle of the track. In contrast, the roll angle differs depending on the speed and type of train. Fortunately, the roll angle is relatively small (a few degrees) and hence $\mathbf{R}_n^b(k) \approx \mathbf{I}$. This is an important simplification that allow to get rid of $\mathbf{R}_n^b$ in the estimation and enables the mapping of the magnetic field along the railway line with an uncalibrated sensor. The latter statement becomes clear if the magnetic map $\tilde{\mathrm{m}}^b()$ used in the proposed algorithm for simultaneous localization and calibration is defined by the true magnetic map $\mathrm{m}^n(\cdot)$ and the calibration parameters $\tilde{\mathbf{C}}$ and $\tilde{\mathbf{b}}$ of the magnetometer used to create the map

$$\tilde{\mathrm{m}}^b(s_k) = \tilde{\mathbf{C}}\tilde{\mathbf{R}}_n^b(s_k)\,\mathrm{m}^n(s_k) + \tilde{\mathbf{b}}, \tag{5}$$

where $\tilde{\mathbf{R}}_n^b(s_k)$ is the rotation matrix between the navigation frame of the track and the body frame of the magnetometer during map creation, note that this matrix depends on the train positions since the attitude during mapping was not constant. Solving (5) for $\mathrm{m}^n(s_k)$ and plugging in the result for $\mathbf{z}^n$ in the sensor model (1) gives the relation between the uncalibrated map and the measurements

$$\begin{aligned}
\tilde{\mathbf{z}}_k^b &= \mathbf{C}\mathbf{R}_n^b(k)\tilde{\mathbf{R}}_n^b(s_k)^{-1}\tilde{\mathbf{C}}^{-1}(\tilde{\mathrm{m}}^b(s_k) - \tilde{\mathbf{b}}) + \mathbf{b} + \mathbf{n}_k \\
&= \mathbf{C}\Delta\mathbf{R}_n^b(k)\tilde{\mathbf{C}}^{-1}(\tilde{\mathrm{m}}^b(s_k) - \tilde{\mathbf{b}}) + \mathbf{b} + \mathbf{n}_k \\
&= \underbrace{\mathbf{C}\Delta\mathbf{R}_n^b(k)\tilde{\mathbf{C}}^{-1}}_{\bar{\mathbf{C}}(k)}\,\tilde{\mathrm{m}}^b(s_k) + \underbrace{\mathbf{b} - \mathbf{C}\Delta\mathbf{R}_n^b(k)\tilde{\mathbf{C}}^{-1}\tilde{\mathbf{b}}}_{\bar{\mathbf{b}}(k)} + \mathbf{n}_k.
\end{aligned} \tag{6}$$

Equation (6) shows that when the map is recorded with an uncalibrated sensor, the measurement model for simultaneous localization and calibration depends on $\bar{\mathbf{C}}(k)$ and $\bar{\mathbf{b}}(k)$ containing the calibration parameters of the magnetometer used for mapping and the magnetometer used during localization. The relative attitude $\Delta\mathbf{R}_n^b(k)$ between the sensor at the current time step and the sensor during mapping at the current position can be time- and position-variant, which would result in calibration parameters that change over time. For the method proposed in the next section we will require that the calibration parameters are constant or only slowly changing compared to the change in the magnetic field when the train moves, otherwise the calibration might not be possible. Since for trains $\mathbf{R}_n^b(k) \approx \mathbf{I}$ this is fulfilled and we end up with the measurement model

$$\begin{aligned}
\tilde{\mathbf{z}}_k^b &= \mathbf{C}\tilde{\mathbf{C}}^{-1}\,\tilde{\mathrm{m}}^b(s_k) + \mathbf{b} - \mathbf{C}\tilde{\mathbf{C}}^{-1}\tilde{\mathbf{b}} + \mathbf{n}_k \\
&= \bar{\mathbf{C}}\,\tilde{\mathrm{m}}^b(s_k) + \bar{\mathbf{b}} + \mathbf{n}_k,
\end{aligned} \tag{7}$$

which again is a linear model with constant parameters. For the proposed approach $\mathbf{R}_n^b(k) \approx \mathbf{I}$ is not strictly required, it is also sufficient when $\Delta\mathbf{R}_n^b(k)$ is constant. This implies that the sensors in different trains do not have to be mounted with the same attitude as long as the relative attitude is fixed. The simplification of a constant $\Delta\mathbf{R}_n^b(k)$ will not be appropriate for most other applications where the sensor can move more freely, e.g., in a 2-D plane. For these cases it is necessary to also estimate the rotation matrix alongside the position and calibration parameters. Furthermore, the map should be recorded with a calibrated sensor and the sensors attitude should be corrected during mapping. Otherwise, the resulting calibration parameters will depend on the sensor's attitude and therefore will be time-variant. The investigation of the feasibility of simultaneous calibration and localization in higher dimensions will be considered in our future research.

So far the train position s_k was assumed to be known. Since the primary goal in this paper is to estimate the train position based on measurements of an uncalibrated magnetometer this is not realistic. So the problem we are facing is that for position estimation the magnetometer has to be calibrated and to calibrate the magnetometer the train position is required. This results in a chicken or egg problem. In [1] we presented a solution to this problem that will be briefly introduced in the next section.

2. Rao-Blackwellized Particle Filter

To avoid the chicken or egg problem the position and the parameters have to be estimated at the same time in a joint estimator. The idea employed here is strongly related to the FastSLAM algorithm in [8] which is based on a Rao-Blackwellized particle filter see, e.g., [9]. In contrast to SLAM the filter estimates the static calibration parameters instead of static landmarks positions and there is no association problem. Formally the task solved by the particle filter is the estimation of the full posterior probability density function (pdf) $p(\mathbf{x}_{0:k}|\mathbf{Z}_{0:k}, \tilde{\mathrm{m}}^b)$ from time step 0 to k of a state vector $\mathbf{x}$ given all the measurement available at time step k. In the example under consideration the state vector contains the dynamic train state $\mathbf{d}$ and the calibration parameters $\boldsymbol{\theta}$

$$\mathbf{x} = [\mathbf{d} \quad \boldsymbol{\theta}]^T \quad \text{with} \quad \mathbf{d} = [s \quad \dot{s} \quad \ddot{s}]^T \,. \tag{8}$$

The dynamic state $\mathbf{d}$ contains the 1D along-track position of the train on the track s, the speed $\dot{s}$ and the acceleration $\ddot{s}$. As a simple approximation for the train dynamics a constant Wiener acceleration model according to [10] is chosen. The general problem with particle filters is their complexity. A particle filter requires sufficient dense samples in all dimensions of the state space were the true posterior is not vanishing. Particle filters are therefore only suitable for real-time applications when the state space is small. For the state vector in (8) the dimension is 15 which already results in an unfeasible number of particles if only 10 samples or values per dimension are considered. To avoid this problem it is possible to exploit the structure of the estimation problem if it can be divided into a linear and nonlinear part. For simultaneous position and calibration parameter estimation the posterior can be factorized into

$$p(\mathbf{d}_{0:k}, \boldsymbol{\theta}_k|\mathbf{z}_{0:k}, \tilde{\mathrm{m}}^b) = \underbrace{p(\mathbf{d}_{0:k}|\mathbf{z}_{0:k}, \tilde{\mathrm{m}}^b)}_{\text{particle filter}} \underbrace{p(\boldsymbol{\theta}_k|\mathbf{d}_{0:k}, \mathbf{z}_{0:k}, \tilde{\mathrm{m}}^b)}_{\text{Kalman filter}}, \tag{9}$$

where the first factor is a nonlinear estimation problem because the train position s in $\mathbf{d}$ is non linearly related to the measurements by the magnetic field map function m. However, the second factor is a linear estimation problem because $\boldsymbol{\theta}$ is conditioned not only on the map and the measurements but also on the complete history of $\mathbf{d}$. This means the positions where the measurements $\mathbf{z}_{0:k}$ are taken, are assumed to be known for the second factor. This results in the linear estimation problem given by (2) that can be solved recursively with the well known Kalman filter. For pdfs that can be factorized like (9) a Rao-Blackwellized particle filter is applicable.

A Rao-Blackwellized particle filter is a combination of a particle filter that runs for each particle a Kalman filter that solves the linear part of the estimation problem. In this particular example the particle filter estimates the dynamic state $\mathbf{d}$ and runs for each of the particle trajectories a Kalman filter for the calibration parameters. The particle filter can be implemented in a straightforward manor but requires some effort in the weight update. In the weight update step of the particle filter the likelihood of the measurements is required. Since the pdf $p(\mathbf{d}_{0:k}|\mathbf{z}_{0:k}, \tilde{\mathrm{m}}^b)$ of the particle filter is not conditioned on the calibration parameters also the likelihood is not conditioned on them. Therefore the likelihood defined by the measurement model (2) is not computable because it requires the calibration parameters. As described in [1] this problems is solved with a marginalization over the pdf of the parameters given by the Kalman filter estimate of the corresponding particle. The marginalization results in Gaussian likelihood where the uncertainty of the measurement noise and the uncertainty due to the estimated calibration parameters is considered.

For the Kalman filter part one can simply implement the well known filter equations. To lower the computational demands of the Rao-Blackwellized particle filter a decomposition of the Kalman filter should be applied. Even tough running an Kalman filter of dimension 12 on modern computers is not a challenge it becomes challenging when such a filter for possibly thousands of particles has to be updated with each new measurement. To reduce the complexity the 12 dimensional state vector is decomposed. The decomposition is possible due to the constant parameter assumption, the form of the observation model (2)-(3) and the diagonal measurement noise covariance matrix of the magnetometer. In the decomposition the state is divided into three parts that are independent of each other. Each of these four dimensional parts are the calibration parameters that relate the map magnetic field to the measurement of one sensor axis. Therefore instead of one Kalman filter with dimension 12, three Kalman filters with dimension four will give the same result. The three magnetometer axis are therefor calibrated independently from each other. Due to cubic complexity in the state dimension for the naive filter implementation this speeds up the algorithm considerably. Since the measurement noise is diagonal also the weight update of the particles can be performed for each sensor axis individuality. In this way real time processing with a rate of 10 Hz is possible on a notebook processor. A detailed filter implementation with pseudo code is found in [1].

(a) Steam engine and steel cabinet on its back.

(b) Diesel railcar.

Figure 2: (a) The magnetometer on the steam engine is mounted on the back in a steel cabinet as shown in the right part of the picture. (b) In the railcar the same sensor was placed on the floor to the right of the door.

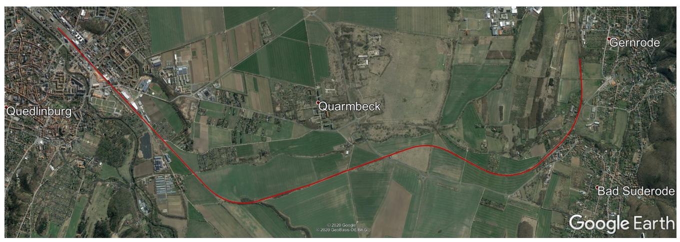

Figure 3: The track in the evaluation is $\approx 7.2\,\mathrm{km}$ long and runs through an rural area between Quedlinburg and Gernrode with mostly open sky view (Map data: Google Earth, GeoBasis-DE/BKG).

IV. MEASUREMENT CAMPAIGN

The data used in this paper was collected from a measurement campaign performed on the track network of the Harzer Schmalspurbahnen. During the campaign measurements with the two different train types shown in Fig. 2 were recorded. Both train types were equipped with a single frequency u-blox LEA-M8T GNSS receiver and a magnetometer contained in an Xsens MTi-G700 inertial measurement unit with nine degrees of freedom. The magnetometer on the steam engine was placed on the back in a steel cabinet. In the railcar, the magnetometer was mounted on the floor. The sensors were centered on the middle of the track and had an height of roughly $1.5\,\mathrm{m}$ in the steam engine and $1\,\mathrm{m}$ in the railcar. The railcar and the steam engine traveled at speeds $\leq 50\,\mathrm{km/h}$. The evaluation is based on a $7.2\,\mathrm{km}$ long track segment between Quedlinburg and Gernrode. A satellite image of the track is shown in Fig. 3. The magnetic field in the map is recorded with the magnetometer data from the steam engine. During the map creation the ground truth is obtained from the GNSS receiver. In the map creation the GNSS speed is integrated to transform the magnetometer measurement time series into a series were each element has a 1D along-track position on the track assigned to it. Based on the assigned along-track positions a linear combination of equally spaced Gaussian basis functions with a fixed bandwidth is fitted to the magnetic field measurement series. This results in a smooth magnetic field map. After this approximation is performed the approximation is sampled at a equidistant grid with a spacing of $\Delta s = 10\,\mathrm{cm}$. The final map is therefore an array that contains the magnetic vector for each (discrete) along-track position on the track. In addition the corresponding ECEF position from the GNSS receiver is stored. The access to the map is than performed by indexing. The index I_k for a certain position s_k is found by $I_k = \mathrm{round}(s_k/\Delta s) + 1$ assuming the first array index is 1.

V. RESULTS

The results shown in this section are calculated with $N_p = 2000$ particles. The map is created with the steam engine magnetic field and for localization the magnetometer measurements of the railcar are used. The filter is implemented in MATLAB and was running in real-time on a conventional notebook processor at a rate of $10\,\mathrm{Hz}$. In the evaluation, 100 Monte Carlo runs were performed to make sure the particle filter convergences for different realization of the process noise used in the prediction step. The shown results are based on the Monte Carlo run that resulted in the highest RMSE of the position.

To evaluate the position accuracy we calculate the Euclidean distance between the ECEF position from the GNSS receiver of the diesel train to the ECEF values stored in the map at the along-track position estimated by the particle filter. The error is based on the minimum-mean-square-error (MMSE) estimate $\hat{s}_{\mathrm{MMSE}}$ of the along-track position that is calculated from the particles

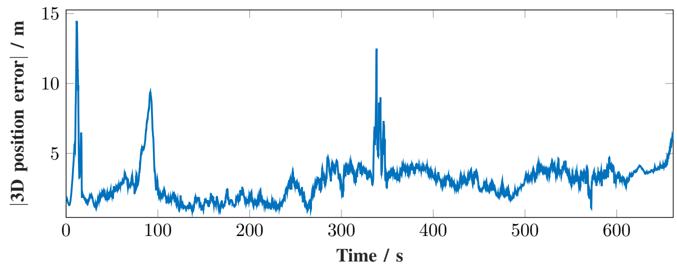

Figure 4: Absolute 3D position error relative to GNSS “ground truth”.

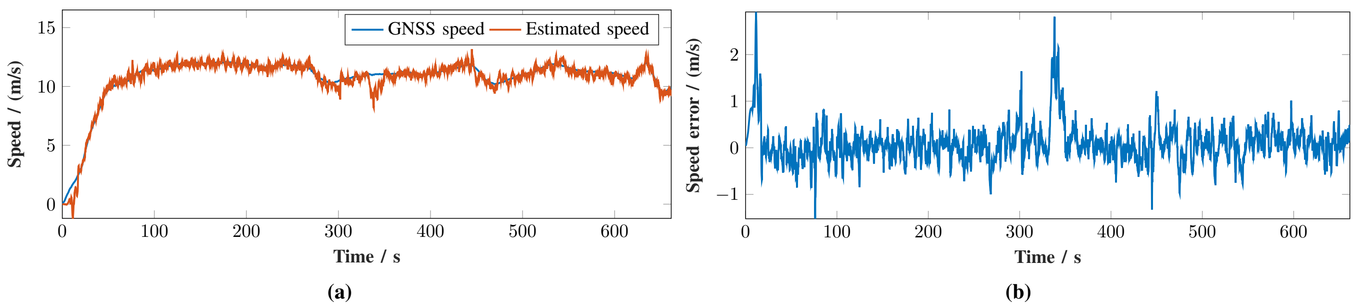

Figure 5: (a) Absolute speed from GNSS and MMSE speed estimate of the particle filter. (b) Speed error relative to GNSS.

and the weights

$$\hat{s}_{\mathrm{MMSE}}(k) = \sum_{i=1}^{N_p} w_k^i s_k^i \quad (10)$$

were w_k^i is the weight of particle i and s_k^i is its along-track position. The same is done for the estimated speed. In Fig. 4 the absolute 3D position error is shown over the whole $661\,\mathrm{s}$ long data set. The position error is below $5\,\mathrm{m}$ for most of the time with some larger errors in the beginning and in the middle. Overall an RMSE of $3.32\,\mathrm{m}$ is achieved. In the beginning the larger error most likely is caused by the not yet fully estimated calibration parameters. In the middle it is not entirely clear were the larger error is coming from but one reason might be the absence of larger, position-dependent, variations of the magnetic field during this time period. When the position dependent variations of the magnetic field are small compared to the sensor noise and time dependent variations caused by vibrations and small attitude changes, the signal to noise ratio becomes too small for accurate estimation. One way to address such problems of temporal inaccuracies is to incorporate an odometer or an inertial measurement unit into the estimation.

In Fig. 5a the estimated speed is compared to the GNSS speed and in Fig. 5b the resulting error is shown. The speed error is mostly below $1\,\mathrm{m/s}$ with some few larger values up to $3\,\mathrm{m/s}$, occurring during the time period when large position errors are observed. As for the position, higher accuracy can be maintained by using additional sensors. Nevertheless, an RMSE of $0.41\,\mathrm{m/s}$ was achieved. For completeness it should be also mentioned that the used GNSS “ground truth” itself is not perfect due to noise and multipath that might contribute to the larger errors.

To show the performance of the calibration, first in each time step the MMSE estimates of the calibration parameters are calculated, second the magnetic field in the map is calibrated to the sensor reading with the MMSE estimate. The resulting magnetic field values are shown in Fig. 6a. The uncalibrated map and the measurements are affected by a large initial misalignment between the sensors in the steam engine and the railcar. In this example the x- and z-axis are switched and inverted. During the evaluation the misalignment was left uncorrected to show that the algorithm is able to also cope with a large misalignment. In practice such large misalignment should be compensated before when possible because the misalignment might lead to longer convergence times and possible divergence. Nevertheless, in the particular example investigated in this paper convergence was not an issue. Fig. 6a shows that after calibration the magnetic field of the map and the measurements follow each other and the large misalignment is compensated. The calibration works not equally well for all axes, while the x- and z-axes data of the calibrated map and the sensor are tightly following each other in the y-axis larger differences are observed as shown in Fig. 6b which shows a zoomed in version of Fig. 6a. Such behavior was not observed in [1] where measurement of

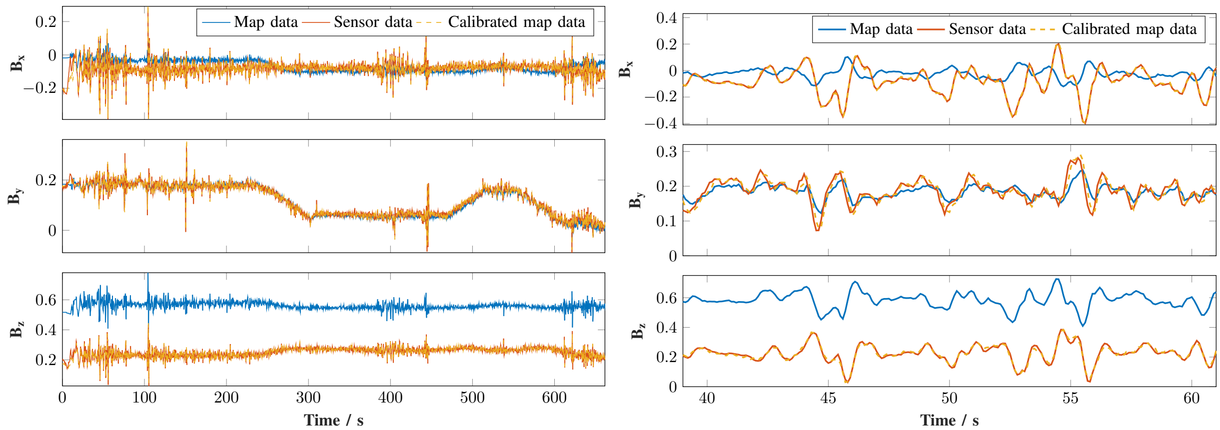

(a) **(b)**

Figure 6: (a) Comparison between the measured magnetic field and the magnetic field in the map before and after calibration at the MMSE position estimate $\hat{s}_{\text{MMSE}}$ of the particle filter. (b) Detailed view of measured magnetic field and the magnetic field in the map before and after calibration from 40 s to 60 s.

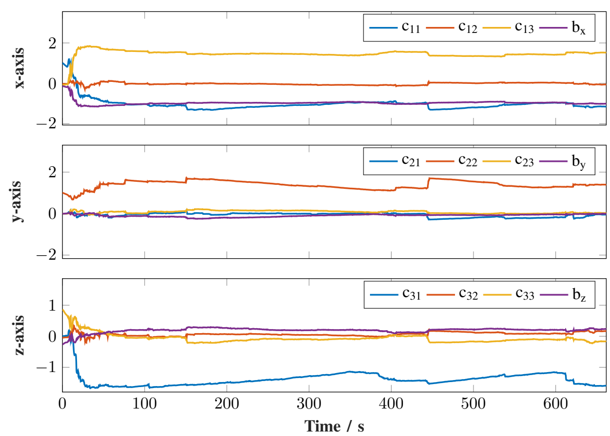

Figure 7: MMSE estimate of calibration parameters for the three magnetometer axis. Each plot corresponds to the estimated state vector of one Kalman filter.

a model train were used. Possible reasons why the y-axis calibration is worse will be discussed in the end of the section.

In Fig. 7 the MMSE estimate for the calibration parameters estimated by the Kalman filters are shown. Interestingly the parameters change considerably over time which was not observed with the model train measurements. We suspect that the changing parameters are caused by different effects. In contrast to the measurements used in this paper the lab measurement were performed with a model train that has no suspension and hence fulfilled the assumption leading to (7) almost perfectly. Furthermore, during the experiments with the model trains the sensors were mounted always at the same height which is not the case for the steam and the diesel train. Since at different heights the magnetic field can look different this can lead to some difficulties during calibration. Another problem that can be encountered in practice is that the “magnetic environment” of the sensors changes over time due to same moving part in the train like gearboxes. Investigating the exact cause is not trivial since the true calibration parameters are unknown. For that we plan to conduct additional measurements in the future. Even though the estimated calibration parameters are not perfect the results clearly show that the estimate is good enough to achieve a high accuracy especially if we consider that only a low-cost magnetometer and nothing else is used. In addition estimating the calibration parameters online during localization has the benefit that the parameters can be adapted to changes in the magnetometers surrounding.

VI. CONCLUSIONS

In this paper, the feasibility of magnetic localization for trains was shown using solely measurements of an uncalibrated magnetometer. This was possible due to the simultaneous localization and calibration algorithm introduced in our prior work [1]. The algorithm is based on a Rao-Blackwellized particle filter that exploits conditional linearity of the calibration parameters given the train position. This reduced the amount of required particles and speeds up the calculations. To further lower the complexity, the Kalman filter part that estimates the calibration parameters is decomposed into three Kalman filters with lower dimensionality. This enables real-time processing of the algorithm with an update rate of $10\,\mathrm{Hz}$.

The accuracy of the position and speed estimation is evaluated with an $\approx 11\,\mathrm{min}$ long data set. For the evaluation, the map was created with a magnetometer in a steam engine while the data set for localization was recorded with a diesel railcar. Despite some sporadic larger errors, an accuracy of the position below $5\,\mathrm{m}$ and an accuracy of the speed below $1\,\mathrm{m/s}$ was achievable. This is already close to the accuracy of the used single frequency GNSS "ground truth". The quality of the calibration was evaluated only qualitatively since it is not the primary object of interest and the true calibration is unknown. But the results clearly show that even though the sensors in the two trains had a large initial misalignment, scaling and offset errors, the filter was able to match the measured magnetic field nicely to the map.

ACKNOWLEDGMENTS

We want to thank the Harzer Schmalspurbahnen and their staff for the support during the measurements.

REFERENCES

[1] B. Siebler, S. Sand, and U. D. Hanebeck, "Localization with Magnetic Field Distortions and Simultaneous Magnetometer Calibration," *IEEE Sensors Journal*, pp. 1–1, 2020, conference Name: IEEE Sensors Journal.

[2] J. Marais, J. Beugin, and M. Berbineau, "A Survey of GNSS-Based Research and Developments for the European Railway Signaling," *IEEE Transactions on Intelligent Transportation Systems*, vol. 18, no. 10, pp. 2602–2618, Oct. 2017.

[3] O. Heirich, B. Siebler, and E. Hedberg, "Study of Train-Side Passive Magnetic Measurements with Applications to Train Localization," 2017. [Online]. Available: https://www.hindawi.com/journals/js/2017/8073982/abs/

[4] B. Siebler, O. Heirich, S. Sand, and U. D. Hanebeck, "Joint Train Localization and Track Identification based on Earth Magnetic Field Distortions," in *2020 IEEE/ION Position, Location and Navigation Symposium (PLANS)*, Apr. 2020, pp. 941–948, iSSN: 2153-3598.

[5] B. Gozick, K. P. Subbu, R. Dantu, and T. Maeshiro, "Magnetic Maps for Indoor Navigation," *IEEE Transactions on Instrumentation and Measurement*, vol. 60, no. 12, pp. 3883–3891, Dec. 2011.

[6] B. Siebler, O. Heirich, and S. Sand, "Train Localization with Particle Filter and Magnetic Field Measurements," in *2018 21st International Conference on Information Fusion (FUSION)*, Jul. 2018, pp. 1–5.

[7] M. Kok and T. B. Schön, "Magnetometer Calibration Using Inertial Sensors," *IEEE Sensors Journal*, vol. 16, no. 14, pp. 5679–5689, Jul. 2016.

[8] M. Montemerlo, S. Thrun, D. Koller, and B. Wegbreit, "FastSLAM: A Factored Solution to the Simultaneous Localization and Mapping Problem," in *National Conference on Artificial Intelligence (AAAI-02)*, 2002.

[9] K. Murphy and S. Russell, "Rao-Blackwellised Particle Filtering for Dynamic Bayesian Networks," in *Sequential Monte Carlo Methods in Practice*, A. Doucet, N. Freitas, and N. Gordon, Eds. New York, NY: Springer New York, 2001, pp. 499–515.

[10] Y. Bar-Shalom, X. R. Li, and T. Kirubarajan, *Estimation with applications to tracking and navigation: theory algorithms and software*. John Wiley & Sons, 2004.